sciendo ASIAN BIOMEDICINE DOI 10.1515/abm-2019-0052 — Asian Biomed (Res Rev News) 2019; 13(4):131–139

**Original article** **Open access**

# (2*E*)-2-Benzylidene-4,7-dimethyl-2,3-dihydro-1*H*-inden-1-one (MLT-401), a novel arylidene indanone derivative, scavenges free radicals and exhibits antiproliferative activity of Jurkat cells

Prasanna Rajagopalan[1,*], Harish C. Chandramoorthy[2,3]

## Abstract

**Background:** The arylidene indanone scaffold has contributed many lead molecules in chemotherapeutic anticancer agent research.

**Objectives:** To determine the oxidant-scavenging activities and antiproliferative activity of (2*E*)-2-benzylidene-4,7-dimethyl-2,3-dihydro-1*H*-inden-1-one (MLT-401), an arylidene indanone derivative.

**Methods:** Jurkat cells, primary lymphocytes, and Vero cells were treated with MLT-401. Antioxidant properties of MLT-401 were determined using 2,2-diphenyl-1-picrylhydrazyl (DPPH)-based, 2,2′-azino-bis-(3-ethylbenzothiazoline-6-sulphonic acid) diammonium salt (ABTS)-based, and ferric-reducing antioxidant potential (FRAP) assays. Inhibition of cell proliferation was determined using a 3-(4,5-dimethylthiazol-2-yl)-2,5-diphenyltetrazolium bromide-based assay. Nuclear status was determined using a DNA fragmentation assay, and cell cycle stage was analyzed by flow cytometry. Mitochondrial membrane enzyme activities were measured using colorimetric methods.

**Results:** The antioxidant assays gave MLT-401 half maximal inhibitory concentration ($IC_{50}$) values of 1611 nM (DPPH-based assay), 2115 nM (ABTS-based assay), and 1586 nM (FRAP assay). MLT-401 inhibited proliferation of Jurkat cells with a concentration for 50% of maximal inhibition of cell proliferation ($GI_{50}$) of 341.5 nM, being 12- and 9-fold less than $GI_{50}$ concentrations for normal lymphocytes and Vero cells, respectively. MLT-401 caused nuclear fragmentation and DNA laddering as seen by electrophoresis. Jurkat cells showed a time-dependent accumulation of sub $G_0/G_1$ cells after MLT-401 treatment. Mitochondrial membrane-bound $Na^+/K^+$ ATPase, $Ca^{2+}$ ATPase, and $Mg^{2+}$ ATPase activities were inhibited by MLT-401 in a dose-dependent manner.

**Conclusion:** MLT-401 possesses significant antiproliferative activity and scavenges free radicals released through mitochondrial membrane damage in a Jurkat cell line model of cancer cells. Further investigation of MLT-401 as a chemotherapeutic anticancer agent and development of other arylidene indanone analogues are warranted. A detailed elucidation of mechanistic pathways is required for further development.

**Keywords:** antioxidants; antitumor drugs; antitumor drug screens; ATPases; indanones

***Correspondence to: Prasanna Rajagopalan,** Department of Clinical Laboratory Sciences, College of Applied Medical Sciences, King Khalid University, Abha 61421, Saudi Arabia, e-mail: rajagopalan@kku.edu.sa

[1]Department of Clinical Laboratory Sciences, College of Applied Medical Sciences, King Khalid University, Abha 61421, Saudi Arabia

[2]Center for Stem Cell Research, College of Medicine, King Khalid University, Abha 61421, Saudi Arabia

[3]Department of Microbiology and Clinical Parasitology, College of Medicine, King Khalid University, Abha 61421, Saudi Arabia

ASIAN BIOMEDICINE

Oxidative stress usually occurs as an imbalance between the production of free radicals and the ability of the body to counteract or detoxify their harmful effects by scavenging or neutralizing them with antioxidants that convert free radicals, and their derivatives such as $H_2O_2$, to benign molecules. Excessive free radical production with low antioxidant defense leads to many pathophysiological conditions [1]. The antioxidants present in normal physiological conditions counteract the free radicals such as reactive oxygen species (ROS) by scavenging them, and thus protecting the body against oxidative damage. Free radicals are considered the main cause of various diseases such as cancer. Unmanaged free radicals lead to development of resistance to multiple drugs in tumor cells and have become a major threat to public health in context of relationships that exist between free radicals and cancers [2]. Chemotherapy considerably improves survivals rates and stops further spread of cancer cells, however, is mostly restricted by its toxic side effects [3]. Because of the resistance that malignant cells accumulate against anticancer drugs, there is great interest in the search for new therapeutic agents [4]. The development of high throughput and high content screening has resulted in many synthetic chemical compounds tested for bioactivity in vitro. These chemical compounds add value in the current drug research with focus on effective, economical, and less toxic drugs.

Arylidene and its derivatives are well known for their antituberculosis activity [5, 6], inhibition in the cell cycle of Src homology region 2 domain-containing phosphatase-2 (SHP-2), a nonreceptor tyrosine-protein phosphatase encoded by *PTPN11* [7], molluscicidal activity [8], antidegenerative activity [9], and hypoglycemic and hypolipidemic activities [10]. Compounds synthesized by combining arylidene indanone scaffolds have increased cytotoxic potencies [11, 12, 13].

The search for biologically active compounds with a safe therapeutic margin has been the key focus of drug discovery in recent years [14, 15].

Briefly, arylidene molecules were functionally modified as derivatives and synthesized. Many are available as commercial chemical molecules and some are synthesized depending on the prediction made using cheminformatics software. A few arylidene derivatives have been synthesized based on their structure–activity relationships (SARs), which are to be explored further for biological activities [15, 16]. From earlier reports and SARs of analogs, we initially screened these molecules for their antioxidant properties. The antioxidant capacity of any compound can be determined in vitro through either hydrogen atom transfer (HAT) or single electron transfer (SET) methods. The HAT method uses the capacity of the compound to scavenge free radicals by hydrogen donation to form a stable compound, while the SET method is based on the ability of compound to transfer 1 electron to reduce compounds including metals, carbonyls, and radicals [17]. The ferric-reducing antioxidant potential (FRAP) assay involves the SET method, while the 2,2-diphenyl-1-picrylhydrazyl (DPPH) and 2,2′-azino-bis-(3-ethylbenzothiazoline-6-sulphonic acid) diammonium salt (ABTS) assays involve both methods, predominantly the SET method [18]. The use of at least 2 different assays to evaluate antioxidant activity of compounds has been recommended by Moon and Shibamoto [19].

To our knowledge, there is no evidence in the literature for these compounds exhibiting antioxidant activity together with antiproliferative activity. Therefore, the present investigation aims to screen a promising arylidene indanone derivative for its antioxidant properties and to further test this lead molecule for its antiproliferative effect on a cancer cell line.

## Materials and methods

All chemicals used in this study were of analytical grade or higher. Cells lines Vero (CRL 1857, normal epithelial cells) and Jurkat (TIB-152, acute T-cell leukemia) were obtained from the American Type Culture Collection. Dulbecco's modified Eagle's medium (DMEM), Roswell Park Memorial Institute (RPMI)-1640 medium, penicillin and streptomycin, nonessential amino acids (NEAA), sodium pyruvate, L-glutamine, 4-(2-hydroxyethyl)-1-piperazineethanesulfonic acid (HEPES) buffer, 2-mercaptoethanol, and fetal bovine serum (FBS) were purchased from Hi Media, Sigma-Aldrich, and Gibco-Invitrogen (India). *p*-iodonitrotetrazolium violet, doxorubicin, DPPH, 3-(4,5-dimethylthiazol-2-yl)-2,5-diphenyltetrazolium bromide (MTT), puromycin, ABTS, and dimethyl sulfoxide (DMSO) were sourced from Sigma-Aldrich. Molecular weight ladders were from Roche. The NucleoSpin DNA extraction kit was from Macherey-Nagel. Guava Cell Cycle Reagent was obtained from Millipore. All other chemicals were procured from Sigma-Aldrich.

### Arylidene indanone derivative MLT-401

The structure of the arylidene indanone derivative (2*E*)-2-benzylidene-4,7-dimethyl-2,3-dihydro-1H-inden-1-one (internal code No. MLT-401) is shown in **Figure 1**. MLT-401 used in the present study was a kind gift from Dr. Radhakrishnan Suresh (Research Scientist, Piramal Enterprises, Chennai, Tamil Nadu, India) and had been synthesized using a slight modification of a method reported previously [20]. In brief, arylidene

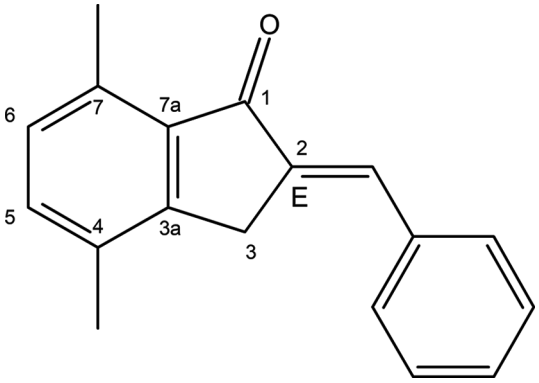


**Figure 1.** Chemical structure of (2*E*)-2-benzylidene-4,7-dimethyl-2,3-dihydro-1*H*-inden-1-one (MLT-401) ($C_{18}H_{16}O$), molecular weight 248.32

molecules had been functionally modified as derivatives and synthesized as reported elsewhere [21]. The MLT-401 used in the present study was 98.9% pure as determined by nuclear magnetic resonance spectroscopy and high-pressure liquid chromatography by Dr. Suresh.

### Cell culture

Cell lines were propagated to 70% confluency (Vero) or density (Jurkat). In brief, the Vero cells were grown in DMEM supplemented with 10% FBS, 100 U/mL penicillin, and 100 µg/mL streptomycin. Using Histopaque (Sigma-Aldrich) density gradient centrifugation, primary lymphocytes were obtained from whole blood in bags that were a kind gift from the central blood bank and contained blood from anonymous normal donor volunteers. The use of the blood from the central blood bank had been approved by the Institutional Review Board of College of Medicine, King Khalid University. T cells were enriched using $CD3^+$ biotin positive selection beads, captured by anti-IgM streptavidin conjugate in Miltenyi Biotec immunomagnetic separation columns. Primary T lymphocytes, and Jurkat cells were grown in RPMI-1640 medium supplemented with 10% FBS, 100 U/mL penicillin and 100 µg/mL streptomycin, 200 mM L-glutamine, 1 mM HEPES, 10 mM NEAA, 100 mM sodium pyruvate, and 0.05 mM 2-mercaptoethanol. Cells (passages 3–12) were maintained in an incubator at 37°C under a humidified atmosphere of 5% $CO_2$. Culture medium was replaced every 2 days, and maintenance was strictly in accordance with standard methods.

### Antioxidant assays

Antioxidant activities were determined using an ABTS assay, DPPH assay for radical-scavenging activity, and an FRAP assay according to methods described previously [22]. After recording the absorbances, antioxidant activity (%) was calculated for each method and results were analyzed using GraphPad Prism software (version 6.0) to calculate half maximal inhibitory concentration ($IC_{50}$) values.

### Cell proliferation assay

A proliferation assay was performed as described by Mosmann [23] with modifications as described as follows. About 5000 cells/well in 100 µL of RPMI-1640 or DMEM media according to the cell type supplemented with 10% FBS and 1% penicillin–streptomycin were plated in triplicate in 96-well microtiter plates. Cells were incubated overnight, and 50 µL of the test compound to meet the desired final concentration was added along with a DMSO blank control. The cells were incubated at 37°C under a humidified atmosphere of 5% $CO_2$ for 72 h. Then, 15 µL of MTT at 5 mg/mL was added and incubation continued for 3.5 h. Media was aspirated from Vero cells, while the plate of Jurkat cells was centrifuged to sediment the cells allowing the media to be removed, before adding MTT in 150 µL of DMSO reading the absorbance at 560 nm with a reference at 640 nm. Percent inhibition was calculated after subtracting MTT absorbance at Day 0. Primary T cells were activated by coating the plates with CD28 antibodies overnight before the T cells were plated for culture. Results were analyzed using GraphPad Prism software (version 6.0).

### DNA fragmentation assay

Jurkat cells were treated with 350 nM MLT-401 for 24, 48, and 72 h. We collected $1 \times 10^6$ cells along with respective controls, centrifuged at 3000 rpm for 5 min and the supernatant aspirated. The cell pellet was washed with ice-cold phosphate-buffered saline (PBS) and resuspended. DNA was isolated using a NucleoSpin DNA extraction kit according to instructions provided by the manufacturer. DNA (2 µg) was mixed with loading and tracking mixture of bromphenol blue (0.25%), xylene cyanol (0.25%) and glycerol (30%) loaded into wells in a 1.6% agarose gel (10 cm × 5 cm and 0.75 cm thick) and separated by electrophoresis at 140–145 V for 1–1.5 h in 1 M Tris, 0.9 M boric acid with 0.01M EDTA, pH 8.0 in a horizontal gel electrophoresis unit (SCIE-PLAS). The separated DNA was stained with 0.5 µg/mL of ethidium bromide, and visualized under ultraviolet light at 302 nm. DNA Molecular Weight Marker III (0.12–21.2 kbp) (Roche, Cat. No. 10 528 552 001) was used in the fragmentation assay.

### Cell cycle assay

Briefly $1 \times 10^6$ of Jurkat cells were washed with PBS. The cells were stained with Guava Cell Cycle reagent according to instructions provided by the manufacturer, and 10,000 events were acquired on a Guava easyCyte flow cytometer. Data were analyzed using Express Pro software (Millipore), and the proportion of the cell population in different cell cycle stages with respect to control was calculated.

### Mitochondrial membrane-bound enzyme assays

Jurkat cells were incubated with 350 nM MLT-401 for 24, 48, or 72 h. The cells were then pelleted, washed once with phosphate buffer, and resuspended the same buffer and frozen. The suspension was thawed to disrupt the cells and cooled on ice. The cell extract was brought to 2.5 mM $MgCl_2$ and centrifuged at 6000 ×*g* for 10 min to remove unbroken cells. The membrane fraction was collected by centrifugation at 50,000 ×*g* for 45 min. After washing twice and rehomogenization in the same buffer (ice cold), the membrane fraction was used to estimate $Na^+/K^+$ ATPase [24], $Ca^{2+}$ ATPase [25], and $Mg^{2+}$ [26].

### Statistical analyses

Experiments were carried out at least in tetrads, and results are expressed as the mean ± standard deviation (SD). Statistical analyses were performed using GraphPad Prism (version 6.0). Concentration for 50% of maximal inhibition of cell proliferation ($GI_{50}$) and $IC_{50}$ values were calculated using a nonlinear regression fit model with variable slope and plotted accordingly. Differences with $P < 0.05$ in tests of statistical inference were considered significant.

## Results

### Antioxidant activity of MLT-401

Several concentrations of MLT-401 were tested for antioxidant activity using ABTS, DPPH, and FRAP assays. $IC_{50}$ values for each of the assays were calculated from the dose–response activities depicted in **Figure 2**. Percent (%) antioxidant activity is plotted against the logarithmic concentrations of MLT-401. The free radical-scavenging activities showed varying levels in a dose-dependent manner. The $IC_{50}$ values

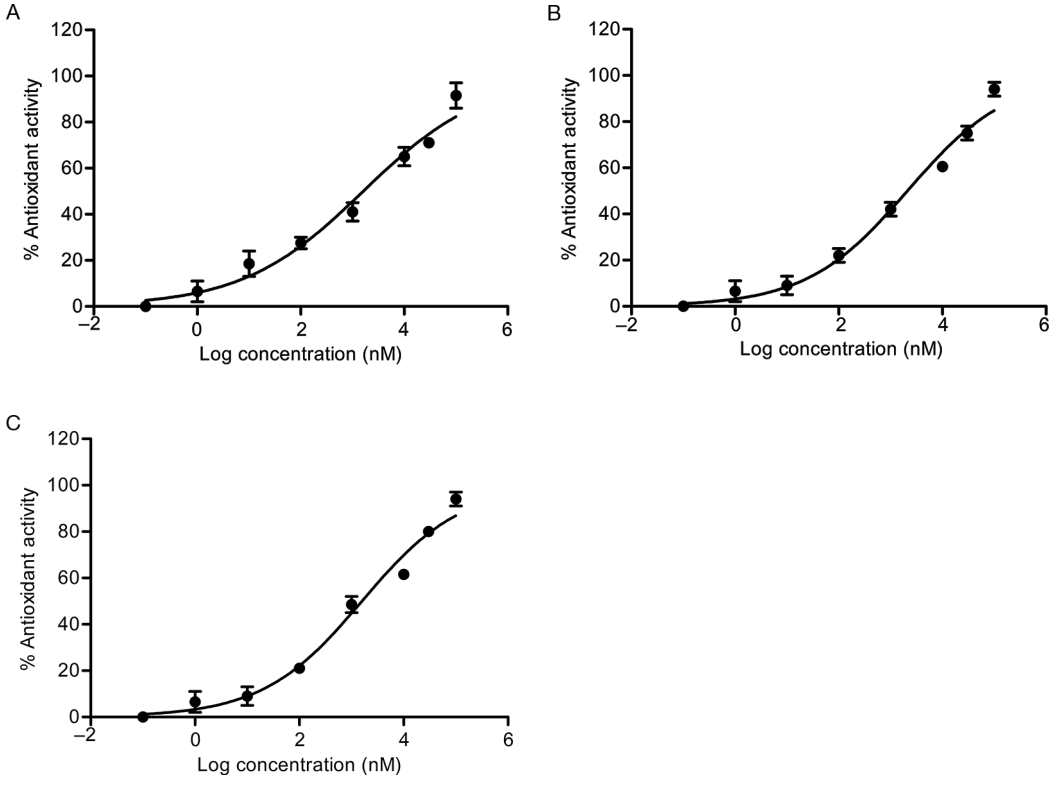


**Figure 2.** Antioxidant profile of (2*E*)-2-benzylidene-4,7-dimethyl-2,3-dihydro-1*H*-inden-1-one (MLT-401). $IC_{50}$ values of the compound for antioxidant properties by (**A**) DPPH assay 1611 nM, (**B**) ABTS assay 2115 nM, and (**C**) FRAP assay 1586 nM

for MLT-401 were 1611 nM (DPPH assay; **Figure 2A**), 2115 nM (ABTS assay; **Figure 2B**), and 1586 nM (FRAP assay; **Figure 2C**).

### Antiproliferative activity of MLT-401

To determine the nontoxic levels of MLT-401 in normal cells and determine its selectivity for cancer cells, we used lymphocytes from normal donors and nontumorigenic Vero cells (adherent cells). MLT-401 inhibited the proliferation of Jurkat cells with $GI_{50}$ value of 341.4 nM (**Figure 3A**). The normal lymphocytes activated with CD28 overnight were inhibited with a $GI_{50}$ value of 4126 nM, while Vero cells were inhibited with a $GI_{50}$ value of 3185 nM (**Figure 3A**), which was in a wide range compared with Jurkat cells. With more than 9-fold potency observed (**Figure 3B**) in inhibiting cancer cell proliferation by comparison with either of the normal cells, we used 350 nM MLT-401 with Jurkat cells for further assays.

### DNA fragmentation activity and cell cycle status after treatment with MLT-401

We found an increase in DNA fragmentation of Jurkat cells, which increased in proportion to time (**Figure 4A**). We assessed the cell cycle status of Jurkat cells at various times after MLT-401 treatment. We found an accumulation of the sub $G_0/G_1$ cell fraction in Jurkat cells treated with 350 nM MLT-401 compared with that in untreated control cells. The proportion of Jurkat cells at the sub-$G_0$ phase increased from 3.2% as observed in the DMSO-treated control cells to 14.4% after treatment with MLT-401 for 24 h (**Figure 4B**). Increasing the treatment time to 48 h and 72 h proportionally increased the percentage of sub-$G_0$ phase cells to 18.6% and 25.1%, respectively (**Figure 4B**).

### Inhibition of mitochondrial membrane-bound enzyme by MLT-401

We observed a significant inhibition of $Na^+/K^+$ ATPase activity in Jurkat cells after MLT-401 treatment (**Figure 5A**). We also observed a reduction in $Ca^{2+}$ ATPase activity (**Figure 5B**) and sustained inhibition of $Mg^{2+}$ ATPase activity in the cells after MLT-401 treatment (**Figure 5C**). The inhibition of all of the membrane-bound ATPases by MLT-401 was dependent on the time of treatment.

## Discussion

MLT-401 showed a significant antiproliferative effect against Jurkat cells. The cytotoxicity of MLT-401 against normal cells was assessed with a Vero cell line and normal primary lymphocytes. A 9–12-fold antiproliferative potency of MLT-401 was found in Jurkat cells compared with that in normal cells indicating the selectivity of MLT-401 for cancer cells. Furthermore, the lack of specificity of MLT-401 for normal cells including Vero cells and normal lymphocytes shows a high selectivity of MLT-401 for cancer cells providing a wide therapeutic window in vitro [17, 27].

ROS are closely related to the induction of apoptosis in cancer cells. Downregulation of ROS by various chemicals blocks initiation of carcinogenesis and/or regulates apoptosis in cancer prevention or therapy [28]. Antioxidants can reverse the multidrug resistance in certain cancer types [28].

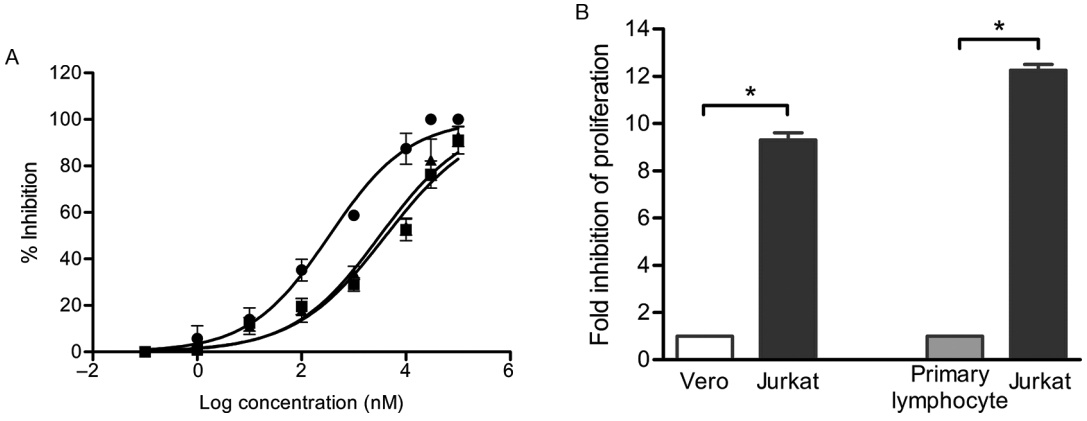


**Figure 3.** (**A**) $GI_{50}$ of (2*E*)-2-benzylidene-4,7-dimethyl-2,3-dihydro-1*H*-inden-1-one (MLT-401) in Jurkat cells (341.4 nM), primary lymphocytes (4126 nM), and Vero cells (3185 nM) showing antiproliferative effects by 3-(4,5-dimethylthiazol-2-yl)-2,5-diphenyltetrazolium bromide (MTT) assay. (**B**) Fold difference in antiproliferative efficacy by MLT-401 between cancer and normal cells was tested. $^{**}P < 0.01$

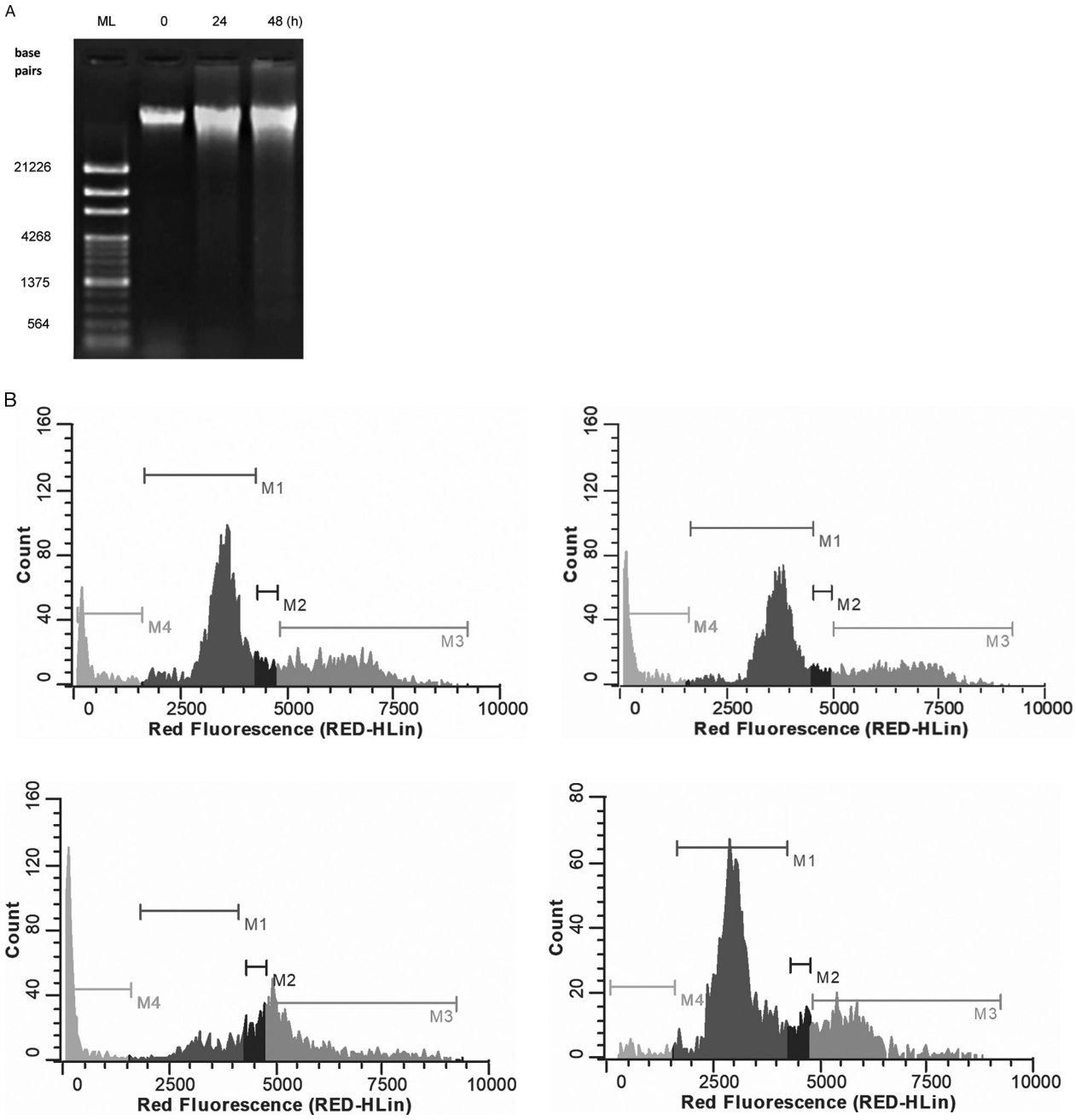


**Figure 4.** Cellular profile after treatment with 350 nM (2*E*)-2-benzylidene-4,7-dimethyl-2,3-dihydro-1*H*-inden-1-one (MLT-401). (**A**) Agarose (1.6%) gel electrophoresis reflecting the presence of DNA fragments on treatment for 0, 24, and 48 h. DNA Molecular Weight Marker III (0.12–21.2 kbp) (Roche, Cat. No. 10 528 552 001) was used in the fragmentation assay. Base pair sizes (ML or marker ladder) are indicated in the Figure. DNA was stained with 0.5 µg/mL of ethidium bromide, and visualized at 302 nm (**B**) Cell cycle changes in Jurkat cells at different times after MLT-401 treatment. Jurkat cells were treated with MLT-401 for 24, 48, and 72 h, and untreated controls were incubated for the same times. Cells were collected after the incubation period, stained with Guava Cell Cycle analysis reagent, and analyzed in a Guava easyCyte flow cytometer to determine the percentage of cells in different phases of the cell cycle. An increase of cells in the sub-$G_0/G_1$ phase was observed with the increase in time of MLT-401 treatment

Arylidene compounds and their derivatives can reverse the multidrug resistance in cancer cells as a result of standard anticancer drugs and act synergistically with the drugs to stop uncontrolled cell proliferation [29]. The observed efficacy of MLT-401 to inhibit the proliferation of cancer cells could therefore be linked to its observed antioxidative properties; however, a detailed study is required to elucidate the mechanisms involved. The efficacy of the MLT-401 as an antioxidant has been suggested for more than 1 method in the present study.

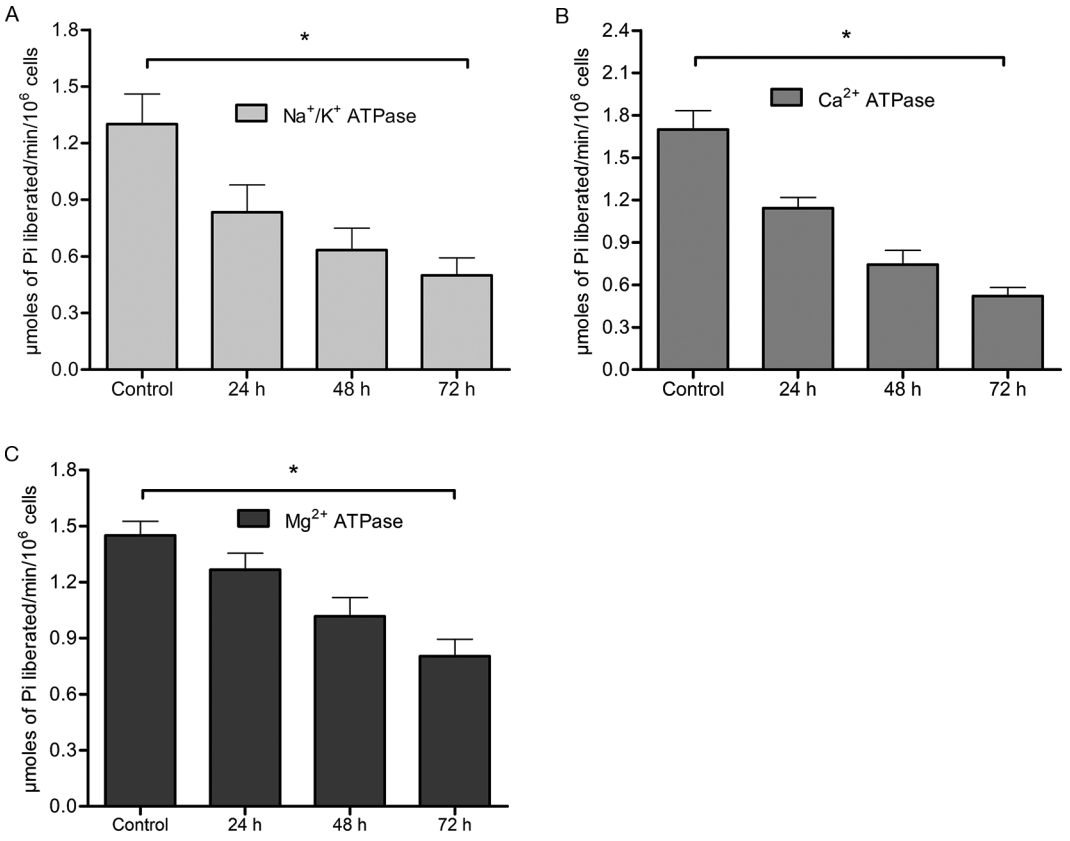


**Figure 5.** The levels of mitochondrial membrane-bound enzyme activities in Jurkat cells treated with 350 nM (2*E*)-2-benzylidene-4,7-dimethyl-2,3-dihydro-1*H*-inden-1-one (MLT-401) at end of 24, 48, and 72 h treatment. (**A**) $Na^+/K^+$ ATPase activity, (**B**) $Ca^{2+}$ ATPase activity, and (**C**) $Mg^{2+}$ ATPase activity. Data represent mean ± standard deviation of 3 individual experiments performed in triplicate. *$P < 0.05$

We extended our study to DNA fragmentation, and our results were consistent with fragmentation indicators of apoptosis [30]. Although apoptosis is a distinct form of programmed cell death, which is usually defective in cancerous cells, the ladder formation we observed is indicative of induced apoptosis [31]. The sub-$G_0/G_1$ cell cycle fraction accumulation further supports induced apoptosis in the Jurkat cells [32]. The oxidant scavenging activity of MLT-401 may be responsible for the gross apoptosis in the Jurkat cells because it alters the malignant physiology of the cells compelling them to undergo apoptosis.

Although apoptosis is distinctive pathway, the involvement of mitochondria in this form of programmed cell death should not be discounted [33]. Our observed inhibition of the mitochondrial membrane-bound $Na^+/K^+$ ATPase may have resulted from depletion of ATP resulting in cytosolic acidification. Therefore, cytosolic rise in $Ca^{2+}$, $Mg^{2+}$, and $Na^+$ with a concomitant decrease in $K^+$ levels may have occurred [34]. Overall, the time-dependent inhibition of membrane-bound ATP enzymes suggests mitochondrial membrane damage caused by MLT-401 in Jurkat cells, leading them to undergo apoptosis.

# Conclusions

MLT-401 is a molecular anticancer candidate that possesses significant antiproliferative activity and scavenges free radicals released through mitochondrial membrane damage in a Jurkat cell line model of cancer cells. Further investigation of MLT-401 as a chemotherapeutic anticancer agent and development of further arylidene indanone analogs are warranted. A detailed elucidation of mechanistic pathways is required for further development.

**Author contributions.** Both authors have contributed substantially to the conception and design of this study; to the acquisition, analysis, and interpretation of the data; and to the drafting and critical revision of the manuscript. Both authors have approved the final version submitted for publication and take responsibility for statements made in the published article.

**Acknowledgments.** The authors are thankful to the Deanship of Scientific Research, King Khalid University, Abha, Saudi Arabia, for the financial support rendered for this study

(R.G.P. 1/80/40). We thank Dr. Radhakrishnan Suresh, Research Scientist, Piramal Enterprises, Chennai 600057, Tamil Nadu, India, for providing us with the gift of MLT-401 used in the present study.

**Conflict of interest statement.** The authors have each completed and submitted an International Committee of Medical Journal Editors Uniform Disclosure Form for Potential Conflicts of Interest. Neither of the authors has any conflict of interest to disclose.

**Data sharing statement.** All data pertaining to the article are presented in the manuscript; raw data on which the statistical summary data presented in the article are based and the NMR data for the MLT-401 are available on reasonable request to the corresponding author for use for noncommercial purposes.

## References

[1] Hoake JB, Pastorino JG. Ethanol, oxidative stress and cytokine-induced liver cell injury. Alcohol. 2002; 27:63–8.

[2] Rahal A, Kumar A, Singh V, Yadav B, Tiwari R, Chakraborty S, Dhama K. Oxidative stress, prooxidants, and antioxidants: the interplay. BioMed Res Int. 2014; 761264. doi:10.1155/2014/761264

[3] Gillet JP, Gottesman MM. Mechanisms of multidrug resistance in cancer. Methods Mol Biol. 2010; 596:47–76.

[4] Schmitz KJ, Otterbach F, Callies R, Levkau B, Hölscher M, Hoffmann O, et al. Prognostic relevance of activated Akt kinase in node-negative breast cancer: a clinicopathological study of 99 cases. Mod Pathol. 2004; 17:15–21.

[5] Fodouop SPC, Simo RT, Amvene JM, Talla E, Etet PFS, Takam P, et al. Bioactivity and therapeutic potential of plant extracts in cancer and infectious diseases. J Dis Med Plants. 2015; 1:8–18.

[6] Özdemir A, Turan-Zitouni G, Kaplancikli ZA, Tunali Y. Synthesis and biological activities of new hydrazide derivatives. J Enzyme Inhib Med Chem. 2008; 29:1–13.

[7] Kaplancikli ZA, Turan-Zitouni G, Ozdemir A, Teulade J-C. Synthesis and antituberculosis activity of new hydrazide derivatives. Arch Pharm Chem Life Sci. 2008; 20:20–8.

[8] Geronikaki A, Eleftheriou P, Vicini P, Alam I, Dixit A, Saxena AK. 2-Thiazolylimino/heteroarylimino-5-arylidene-4-thiazolidinones as new agents with SHP-2 inhibitory action. J Med Chem. 2008; 51:5221–8.

[9] Abdelrazek FM, Metz P, Kataeva O, Jäger A, El-Mahrouky SF. Synthesis and molluscicidal activity of new chromene and pyrano[2,3-*c*]pyrazole derivatives. Arch Pharm. 2007; 340:543–8.

[10] Ottanà R, Maccari R, Ciurleo R, Vigorita MG, Panico AM, Cardile V, et al. Synthesis and in vitro evaluation of 5-arylidene-3-hydroxyalkyl-2-phenylimino-4-thiazolidinones with antidegenerative activity on human chondrocyte cultures. Bioorg Med Chem. 2007; 15:7618–25.

[11] da Costa Leite LF, Veras Mourão RH, de Lima Mdo C, Galdino SL, Hernandes MZ, de Assis Rocha Neves F, et al. Synthesis, biological evaluation and molecular modeling studies of arylidene-thiazolidinediones with potential hypoglycemic and hypolipidemic activities. Eur J Med Chem. 2007; 42:1263–71.

[12] Bansal R, Guleria S. Synthesis of 16*E*-[3-methoxy-4-(2minoethoxy) benzylidene]androstene derivatives as potent cytotoxic agents. Steroids. 2008; 73:1391–9.

[13] Menezes JCJMDS. Arylidene indanone scaffold: medicinal chemistry and structure–activity relationship view. RSC Adv. 2017; 7:9357–72.

[14] Pati HN, Das U, De Clercq E, Balzarini J, Dimmock JR. Molecular modifications of 2-arylidene-1-indanones leading to increased cytotoxic potencies. J Enzyme Inhib Med Chem. 2007; 22:37–42.

[15] Minotti G, Menna P, Salvatorelli E, Cairo G, Gianni L. Anthracyclines: molecular advances and pharmacologic developments in antitumor activity and cardiotoxicity. Pharmacol Rev. 2004 56:185–229.

[16] Carrera MP, Ramírez-Expósito MJ, Martínez-Martos JM. Actual and potential agents and biomarkers in the treatment of cancer. Anti-cancer Agents Med Chem. 2009; 9:500–16.

[17] Rajagopalan P, Alahmari KA, Elbessoumy AA, Balasubramaniam M, Suresh R, Shariff MEA, Chandramoorthy HC. Biological evaluation of 2-arylidene-4, 7-dimethyl indan-1-one (FXY-1): a novel Akt inhibitor with potent activity in lung cancer. Cancer Chemother Pharmacol. 2016; 77:393–404.

[18] Becker K, Schroecksnadel S, Gostner J, Zaknun C, Schennach H, Überall F, Fuchs D. Comparison of *in vitro* tests for antioxidant and immunomodulatory capacities of compounds. Phytomedicine. 2014; 21:164–71.

[19] Moon JK, Shibamoto T. Antioxidant assays for plant and food components. J Agric Food Chem. 2009; 57:1655–66.

[20] Lee HJ, Kim TH, Kim JN. One-pot synthesis of (*E*)-2-arylideneindan-1-ones from the Baylis-Hillman adducts *via* the successive inter- and intramolecular Friedel-Crafts reactions. Bull Korean Chem Soc. 2001; 22:1059–68.

[21] Prasanna R, Harish CC. Anticancer effect of a novel 2-arylidene-4,7-dimethyl indan-1-one against human breast adenocarcinoma cell line by $G_2$/M cell cycle arrest. Oncology Res. 2010; 18:461–8.

[22] Dzoyem JP, Eloff JN. Anti-inflammatory, anticholinesterase and antioxidant activity of leaf extracts of twelve plants used traditionally to alleviate pain and inflammation in South Africa. J Ethnopharmacol. 2015; 160:194–201.

[23] Mosmann T. Rapid colorimetric assay for cellular growth and survival: application to proliferation and cytotoxicity assays. J Immunol Methods 1983; 65:55–63.

[24] Solomson LP, Liepkalns VA, Spector A. Changes in ($Na^+$ + $K^+$)-ATPase activity of Ehrlich ascites tumor cells produced by alteration of fatty acid composition. Biochem. 1976; 15:892–7.

[25] Hjertén S, Pan H. Purification and characterization of two forms of a low-affinity $Ca^{2+}$-ATPase from erythrocyte membranes. Biochem Biophys Acta. 1983; 728:281–8.

[26] White MD and Ralston GB. Purification of water soluble $Mg^{2+}$ ATPase from human erythrocyte membranes. Biochem Biophys Acta.1980; 599:569–79.

[27] Deng M, Zha J, Jiang Z, Jia X, Shi Y, Li P, et al. Apatinib exhibits anti-leukemia activity in preclinical models of acute lymphoblastic leukemia. J Transl Med. 2018; 16:47. doi:10.1186/s12967-018-1421-y

[28] Guo J, Zhang Y, Zhang J, Liang J, Zeng L, Guo G. Anticancer effect of tert-butyl-2(4,5-dihydrogen-4,4,5,5-tetramethyl-3-O-1H-imidazole-3-cationic-1-oxyl-2)-pyrrolidine-1-carboxylic ester on human hepatoma HepG2 cell line. Chem Biol Interact. 2012; 199:38–48.

[29] Kamal A, Hussaini SMA, Malik MS. Recent developments towards podophyllotoxin congeners as potential apoptosis inducers. Anticancer Agents Med Chem. 2015; 15:565–74.
[30] Wang C, Youle RJ. The role of mitochondria in apoptosis. Annu Rev Genet. 2009; 43:95–118.
[31] Majtnerová P, Roušar T. An overview of apoptosis assays detecting DNA fragmentation. Mol Biol Rep. 2018; 45:1469–78.
[32] Babes RM, Tofolean IT, Sandu RG, Baran OE, Cosoreanu V, Ilie MT, et al. Simple discrimination of sub-cycling cells by propidium iodide flow cytometric assay in Jurkat cell samples with extensive DNA fragmentation. Cell Cycle. 2018; 17:766–79.
[33] Lopez J, Tait SW. Mitochondrial apoptosis: killing cancer using the enemy within. Br J Cancer. 2015; 112:957–62.
[34] Gassbarini A, Borle AB, Faghali H, Bender C, Francavilla A, Van Thiel D. Effect of anoxia on intracellular ATP, $Na^{+}_{i}$, $Ca^{2+}_{i}$, $Mg^{2+}_{i}$, and cytotoxicity in rat hepatocytes. J Biol Chem. 1994; 267: 6654–63.